Electronic Supplementary Material (ESI) for Physical Chemistry Chemical Physics

Preparation of polymer-supported Gold Nanoparticles based on resins containing Ionic Liquid-like fragments: Easy control of size and stability

M. Isabel Burguete, Eduardo García-Verdugo,*, Santiago V. Luis,* Julián A. Restrepo.

Synthesis and Characterisation of SILLPs.

General procedure for the synthesis of SILLPs. A Merrifield resin (2 g, 1.1 mmol g^{-1}, 1%DVB) was suspended in 25 mL of the corresponding imidazole. The system was heated at 80 °C. After 3 h, the polymer was filtered, washed with DMF (3 × 20 mL), MeOH (3 × 20 mL), CH_2Cl_2 (3 × 20 mL) and dried under vacuum at 60 ◦C.

- **SILLP 5a**

FT-IR (cm^{-1})-ATR: 3419, 3141, 3060, 2922, 2848, 1567, 1616, 1510, 1449, 1332, 1159, 1022, 823, 761, 706, 661, 619.

Raman (cm^{-1}): 1612, 1579, 1450, 1413, 1385, 1331, 1188, 1160, 1091, 1022, 1001, 831, 765, 716, 664, 642, 620, 411, 332.

Elemental Analysis, experimental: %N 8.49. found: %N 8.91.

- **SILLP 5b**

FT-IR (cm^{-1})-ATR: 3931, 3891, 3830, 3738, 3386, 3147, 3086, 2925, 1644, 1566, 1515, 1451, 1334, 1159, 824, 761, 706, 616.

Raman (cm^{-1}): 1615, 1455, 1415, 1387, 1332, 1192, 1092, 1024, 1004, 836, 769, 669, 646, 624, 414, 358, 270, 149.

Elemental Analysis: experimental: %N 10.44. found: %N 10.62.

- **SILLP 5c**

FT-IR (cm^{-1})-ATR: 3808, 3738, 3624, 3361, 3025, 2921, 1601, 1491, 1448, 1159, 1025, 754, 696.

Raman (cm^{-1}): 1607, 1588, 1456, 1334, 1189, 1161, 1099, 1037, 1008, 802, 768, 629, 553, 418, 283, 236, 127, 101.

Elemental Analysis, experimental: %N 1.95. found: %N 2.83.

- **SILLP 5d**

FT-IR (cm^{-1})-ATR: 3898, 3858, 3741, 3387, 3025, 2922, 1651, 1491, 1449, 1161, 1091, 1023, 828, 758, 700, 619.

Raman (cm^{-1}): 1609, 1589, 1456, 1420, 1335, 1190, 1162, 1102, 1037, 1008, 841, 767, 650, 630, 554, 419, 275, 128.

Elemental Analysis, experimental: %N 3.56. found: %N 3.06.

- **SILLP 6a**

FT-IR (cm^{-1})-ATR: 3741, 3623, 3386, 3060, 2925, 2854, 1741, 1644, 1560, 1515, 1455, 1367, 1276, 1156, 823, 761, 703.

Raman (cm^{-1}): 1614, 1582, 1448, 1420, 1329, 1189, 1157, 1115, 1057, 1026, 1002, 830, 765, 642, 622, 409, 274, 136.

Elemental Analysis, experimental: %N 7.40. found: %N 7.86.

- **SILLP 6b**

FT-IR (cm^{-1})-ATR: 3844, 3738, 3623, 3387,3062, 2930, 2867, 1644, 1514, 1560,1455, 1363, 1156, 852, 761.

Raman (cm^{-1}): 1618, 1569, 1452, 1424, 1333, 1195, 1122, 1062, 1030, 1008, 836, 775, 649, 626, 417, 334, 272, 130.

Elemental Analysis, experimental: %N 9.28. found: %N 9.16.

- **SILLP 6c**

FT-IR (cm^{-1})-ATR: 3842, 3738, 3625, 3360, 3026, 2923, 2848, 1601, 1559, 1492, 1448, 1156, 1025, 754, 696.

Raman (cm^{-1}): 1609, 1590, 1455, 1337, 1205, 1189, 1162, 1038, 1009, 913, 836, 803, 768, 651, 631, 419, 236, 126.

Elemental Analysis, experimental: %N 1.79. found: %N 2.71.

- **SILLP 6d**

FT-IR (cm^{-1})-ATR: 3866, 3742, 3674, 3650, 3623, 3567, 3385, 3026, 2925, 1648, 1560, 1514, 1451, 1157, 758, 700, 616.

Raman (cm^{-1}): 1604, 1584, 1450, 1421, 1328, 1183, 1156, 1063, 1030, 1001, 905, 830, 754, 642, 622, 413, 261, 136.

Elemental Analysis, experimental: %N 3.13. found: %N 2.93.

- **SILLP 7a**

FT-IR (cm^{-1})-ATR: 3845, 3742, 3622, 3384, 3057, 2924, 2853, 1642, 1515, 1454, 1367, 1269, 1182, 769, 702.

Raman (cm^{-1}): 1615, 1512, 1449, 1306, 1187, 1123, 1078, 1031, 1002, 965, 834, 723, 642, 622, 412, 278, 136.

Elemental Analysis, experimental: %N 5.80. found: %N 6.16.

- **SILLP 7b**

FT-IR (cm^{-1})-ATR: 3861, 3829, 3811, 3738, 3680, 3622, 3362, 2925, 2854, 1741, 1691, 1516, 1464, 1426, 1367, 1177, 1040.

Raman (cm^{-1}): 1618, 1515, 1450, 1393, 1309, 1193, 1130, 1086, 1007, 970, 841, 730, 679, 649, 419, 345, 277, 130.

Elemental Analysis, experimental: %N 5.91. found: %N 6.93.

- **SILLP 7c**

FT-IR (cm^{-1})-ATR: 3808, 3738, 3358, 3026, 2922, 2851, 1601, 1492, 1448, 1368, 1026, 754, 696.

Raman (cm^{-1}): 1609, 1589, 1517, 1455, 1338, 1190, 1162, 1078, 1039, 1009, 850, 802, 767, 630, 415, 274, 238, 128.

Elemental Analysis, experimental: %N 1.65. Calculado: %N 2.48.

- **SILLP 7d**

FT-IR (cm^{-1})-ATR: 3897, 3858, 3741, 3674, 3650, 3622, 3568, 3386, 3027, 2924, 2853, 1701, 1514, 1451, 1092, 760, 699, 614.

Raman (cm^{-1}): 1609, 1589, 1517, 1455, 1338, 1190, 1162, 1078, 1039, 1009, 850, 802, 767, 630, 415, 274, 238, 128.

Elemental Analysis, experimental: %N 2.46. Found: %N 2.65.

The following figures S1 and S2 depict, as an example, the characterisation of resin **7a** by FTIR-ATR and Raman Microscopy.

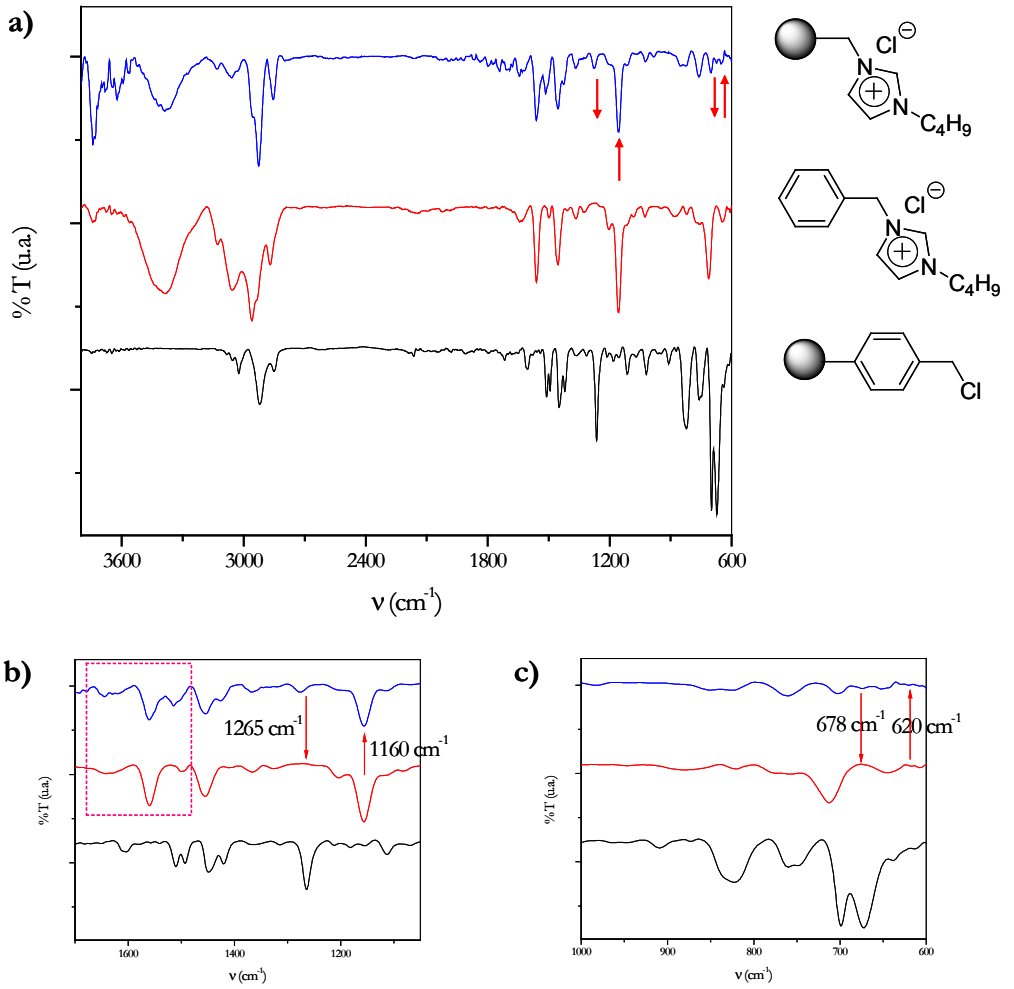

Figure S1. a) FT-IR-ATR spectra of the polymer **7a** and those for **1a** and the related ionic liquid 1-decyl-2methyl-benzyl-imidazolium chloride: a) full spectra; b) 1400-1000 cm^{-1} region; c) 1000-500 cm^{-1} region. The arrows indicate the most significant bands and changes. The sense of the arrow indicates if the bans appears or disappears.

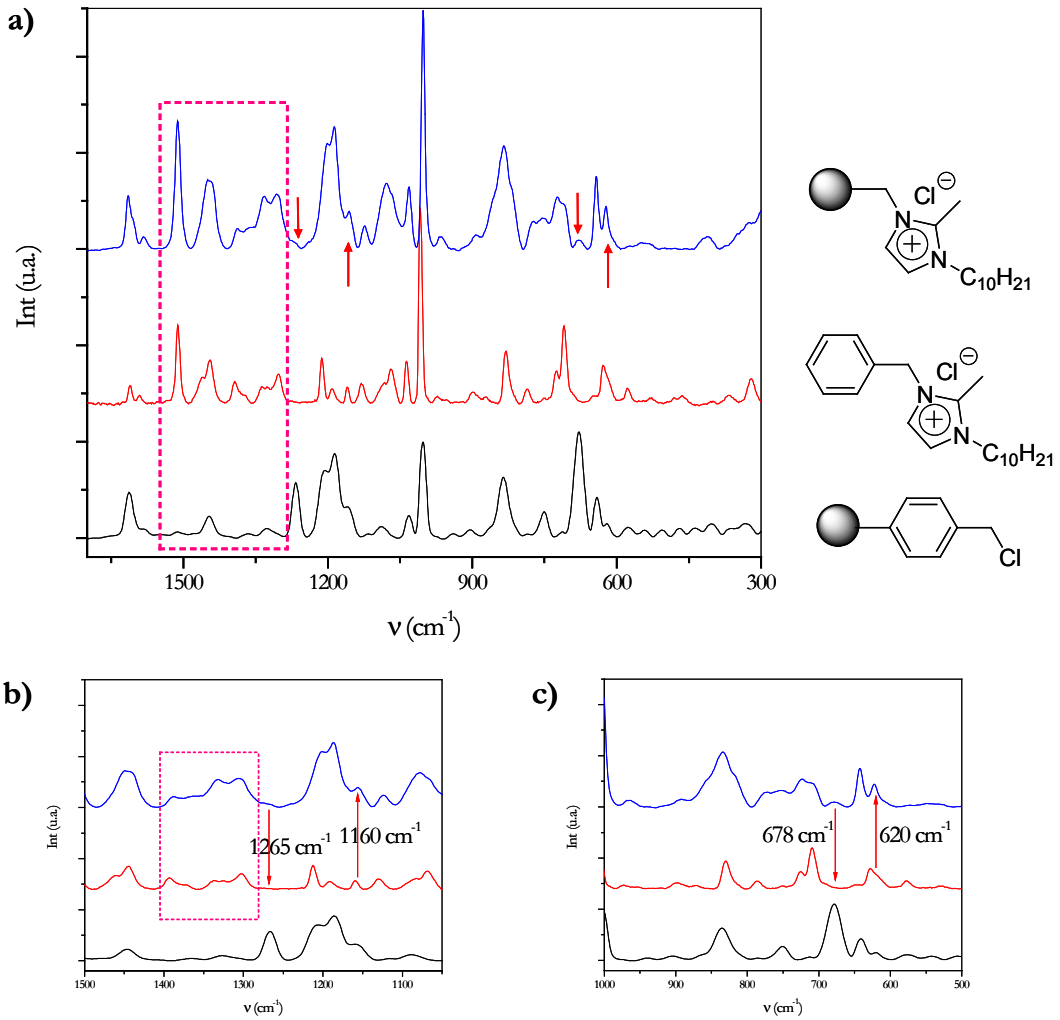

Figura S2. FT-Raman spectra of the polymer **7a** and those for **1a** and the related ionic liquid 1-decyl-2methyl-benzyl-imidazolium chloride. a) full spectra b) 1400-1000 cm^{-1} region. c) 1000-500 cm^{-1} region. The arrows indicate the most significant bands and changes. The sense of the arrow indicates if the bans appears or disappears.

Swelling study.

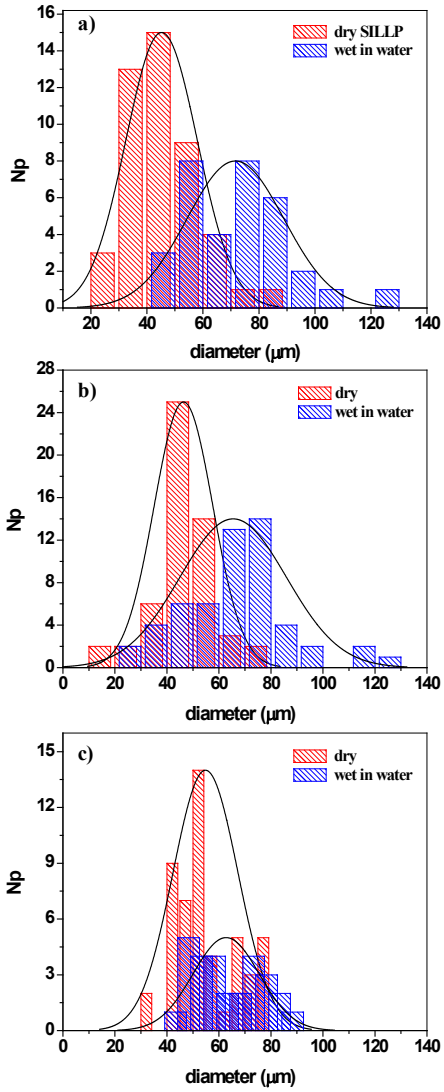

Figure S3. Effect on the swelling degree in water of the substitution for the alkylimmidazolium in the SILLPs a) SILLP-**5a** (R=CH_3 R´=H); b) SILLP-**6a** (R=C_4H_9, R´=H); c) SILLP-**7a** (R= $C_{10}H_{21}$, R´=CH_3). Np= Number of particles.

Synthesis of AuNPs immobilised onto SILLP-5a with different loadings. The corresponding SILLP (100 mg, **5-7**) was suspended in a round bottomed flask containing 2 mL of deionised water. Afterwards, an aqueous solution of the gold precursor ($HAuCl_4$) along with 10 µL of HCl was added and the suspension was stirred for 2 hours at r.t (see Table S1 for the final gold concentration). The polymer was then filtered and washed with water (3 x 1 mL) and methanol (1x 0.75 mL). Finally the polymer (light yellow), was vacuum dried at 60ºC until constant weight.

The Au(III) was reduced to Au(0) by adding an aqueous solution of $NaBH_4$ (1 mL of solution; $NaBH_4$: $AuCl_4$ = 20:1) to a suspension of the different Au(III)-SILLPs (100 mg in 1 mL). The suspension was stirred for to 2 hours at r.t. for completion of the reduction. Afterwards, the polymer was filtered and washed with deionised water (3x2.0 mL) and MeOH (1x1.70 mL). Finally the polymer was vacuum dried at 60ºC till constant weight.

Table S1. Absorption of Au(III) species onto SILLP-**5a**.[a]

Entry	$[AuCl_4^-]$[b]	(%) Uptake[c]	mg Au/g[d]	IL:Au[e]	λ_{max}[f]
1	1.7	>99	9.84	60:1	526
2	5.1	>99	29.6	20.9:1	529
3	8.4	>99	49.4	12.6:1	530
4	16.5	>99	98.5	6.3:1	531
5	32.0	>99	197.4	3.1:1	534
6	60.0	>99	395.4	1.6:1	536
7	84.9	>99	593.1	1.0:1	543
8	99.1	96	694.5	0.9:1	545
9	112.3	89	755.0	0.7:1	547

[a] 200 mg of SILLP-**5a** (total IL-like fragments content 3.03 mmol/g). [b] concentration of $AuCl_4^-$ in mg/mL.[c] calculated by ICP-MS after adsorption. [d] loading of Au-SILLPs in mg Au/g of support. [e] molar ratio IL-like groups/gold. [f] SPR for the AuNPs-SILLPs obtained after reduction.

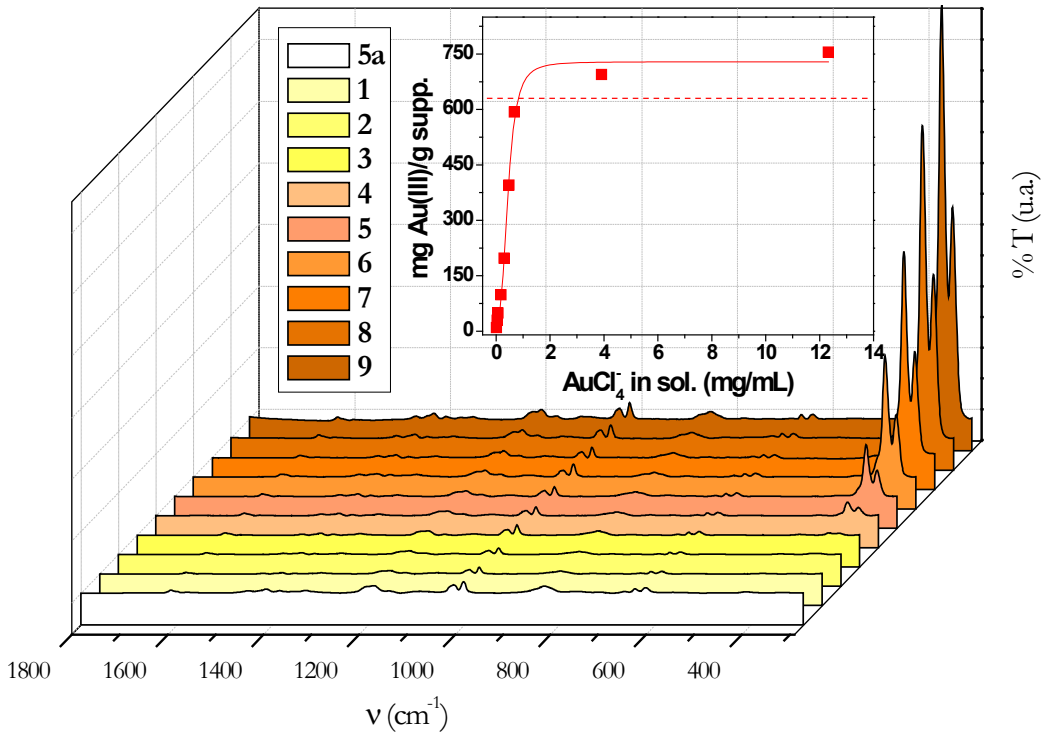

Figure S4 a) Raman spectra of the different Au(III)SILLP ranging from 29 to 755 mg of Au(III)/g b) Adsorption Isotherm of different $AuCl_4^-$ solutions over SILLP-**5a** (concentration ranging from ca. 1.7 to 112 mg/mL of $AuCl_4^-$).

TEM analysis of AuNPs-SILLPs obtained from 8a with different gold loadings

TablaS2. Size distribution for AuNPs-SILLPs obtained from **8a**.

Entry	AuNPs-SILLP	Loading Au (mmol/g.)	d (nm) [a]	S.D. [b]	Np[c]
1	AuNPs-SILLPs-**a**	0.05	4.73	3.2	121
2	AuNPs-SILLPs-**c**	0.25	3.27	1.13	179
3	AuNPs-SILLPs-**f**	2.02	2.52	0.79	149
4	AuNPs-SILLPs-**h**	3.83	2.17	0.77	250

[a] As mean size diameter of all AuNPs analysed.[b] standard deviation. [c] Number of particles took into consideration.

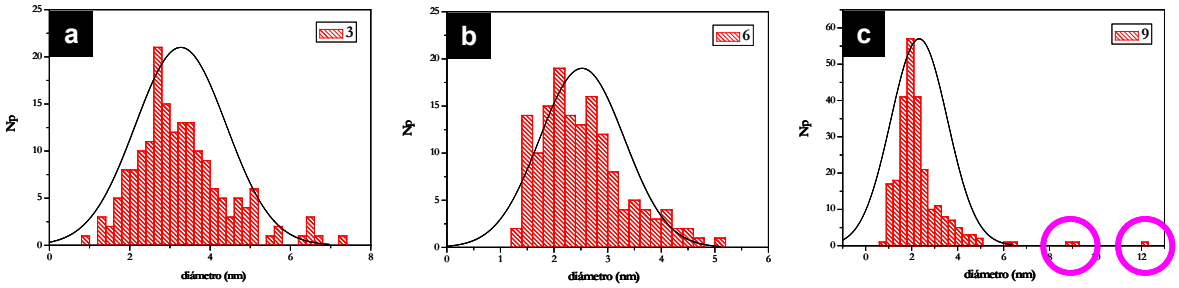

Figure S5. Histograms of the AuNPs size distribution in the AuNPs-SILLPs obtained from 8a having different gold loading **8a** corresponding: a) entry 2 Table S2; b) entry 3 Table S2; c) entry 4 Table S2. Pink circles in Figure c highlight the presence of some particles with much higher particle sizes not corresponding with the normal size distribution observed for most particles.

Synthesis of the AuNPs in solution:

Method i) An aqueous solution of the precursor ($HAuCl_4$) was heated to reflux and then a solution sodium citrate was added. After 5 minutes it could be appreciated the Au(III) reduction to Au(0) associated with a colour change of the solution from yellow to light reddish ,up to turn into completely red-violet. Then the solution was refluxed for 30 min. After this time, the solution was covered to avoid AuNPs aggregation, due to UV light effect, and cooled. Then it was stored in the refrigerator.

Method ii) A sodium citrate solution was added under vigorous stirring to an aqueous solution of the precursor ($HAuCl_4$). After 5 minutes, 1 mL of an aqueous solution of $NaBH_4$ (0.081 wt% solution of $NaBH_4$ dissolved in a 44.75 mM solution of sodium citrate) was slowly added at room temperature for 10 minutes. An immediate change in the colour was observed, changing the yellownish initial solution to red-violet.

Table S3. Preparation AuNPs-SILLPs composites by AuNPs absorption.

Entry	AuNPs solution	TEM (nm)[e]	AuNPs-SILLPs[f]	DR-UV-Vis. (nm)	TEM (nm)
1	AuS_1[a]	9±2	**a** (*g*)	523	162 ±180
2	AuS_2[b]	9±3	**b** (*g*)	538	106 ±143
3	AuS_3[c]	6.5±1.4	**c** (*g*)	525	90 ± 65
4	AuS_4[d]	17±3	**d** (*g*)	547	96 ± 59

[a] reducing agent $NaBH_4$, r.t. 0.5M, Au:citrate 1:1.25 molar ratio. [b] reducing agent $NaBH_4$, r.t. 0.24M, Au:citrate 1:6 molar ratio. [c] reducing agent $NaBH_4$, r.t. 0.5M, Au:citrate 1:1.25 molar ratio. [d] without any additional reducing agent , 117°C,. 0.25M, Au:citrate 1:9 molar ratio. [e]The UV-visble solution showed a plasmon AuNPs band at ca. 526 nm. [f] all the solutions were adsorbed onto 100 mg of SILLPs-**5a** to yield AuNPs-SILLPs-**9a-d** with a loading of 0.0507 mmol/g of support.

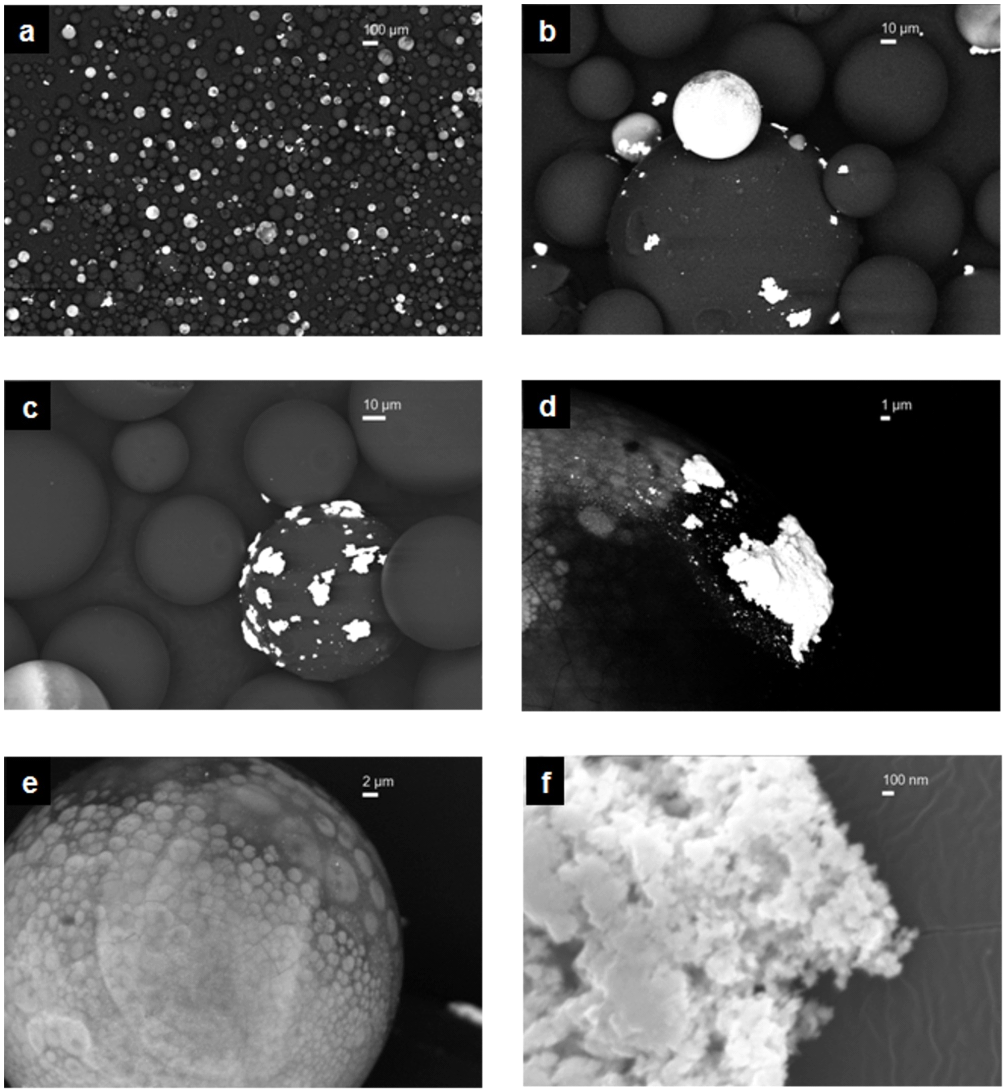

Figure S6. SEM images for the composites obtained when a solution of $AuCl_4^-$ was reduced in the presence of the SILLP **5a.**

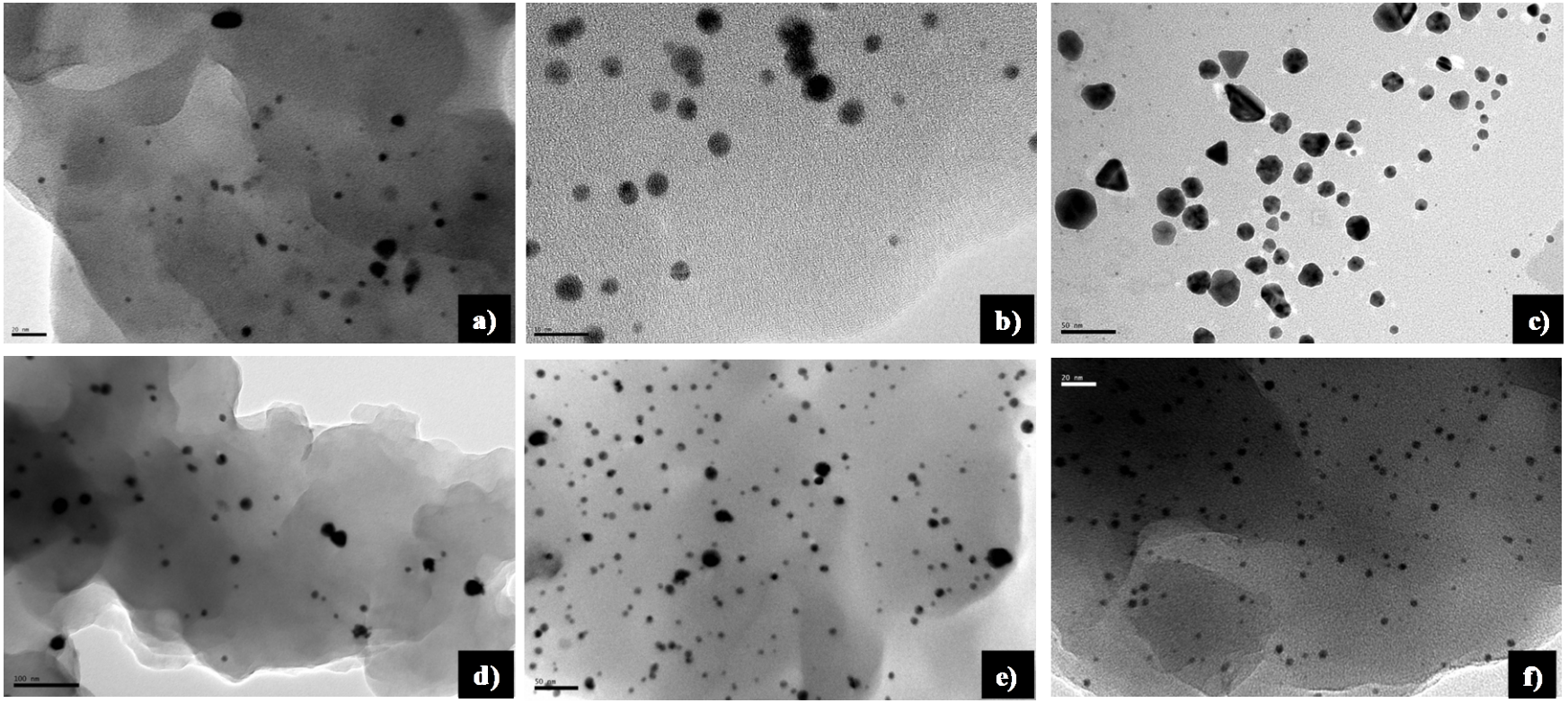

Figure S7. TEM images of different AuNPs-SILLPs prepared by the loading/reduction procedure using resins having a high loading of IL-like moieties: a) AuNPs-SILLP-**11a** (R=CH_3, R´=H) (bar 20nm), b) AuNPs-SILLP-**12a** (R=C_4H_9, R´=H) (bar 10 nm), c) AuNPs-SILLP-**13a**, (R= $C_{10}H_{21}$, R´=CH_3) (bar 50nm), d) AuNPs-SILLP-**11b** (R=CH_3, R´=H) (bar 100 nm), e) AuNPs-SILLP-**12b** (R=C_4H_9, R´=H) (bar 50 nm), and f) AuNPs-SILLP-**13b**, (R= $C_{10}H_{21}$, R´=CH_3) (bar 20 nm).

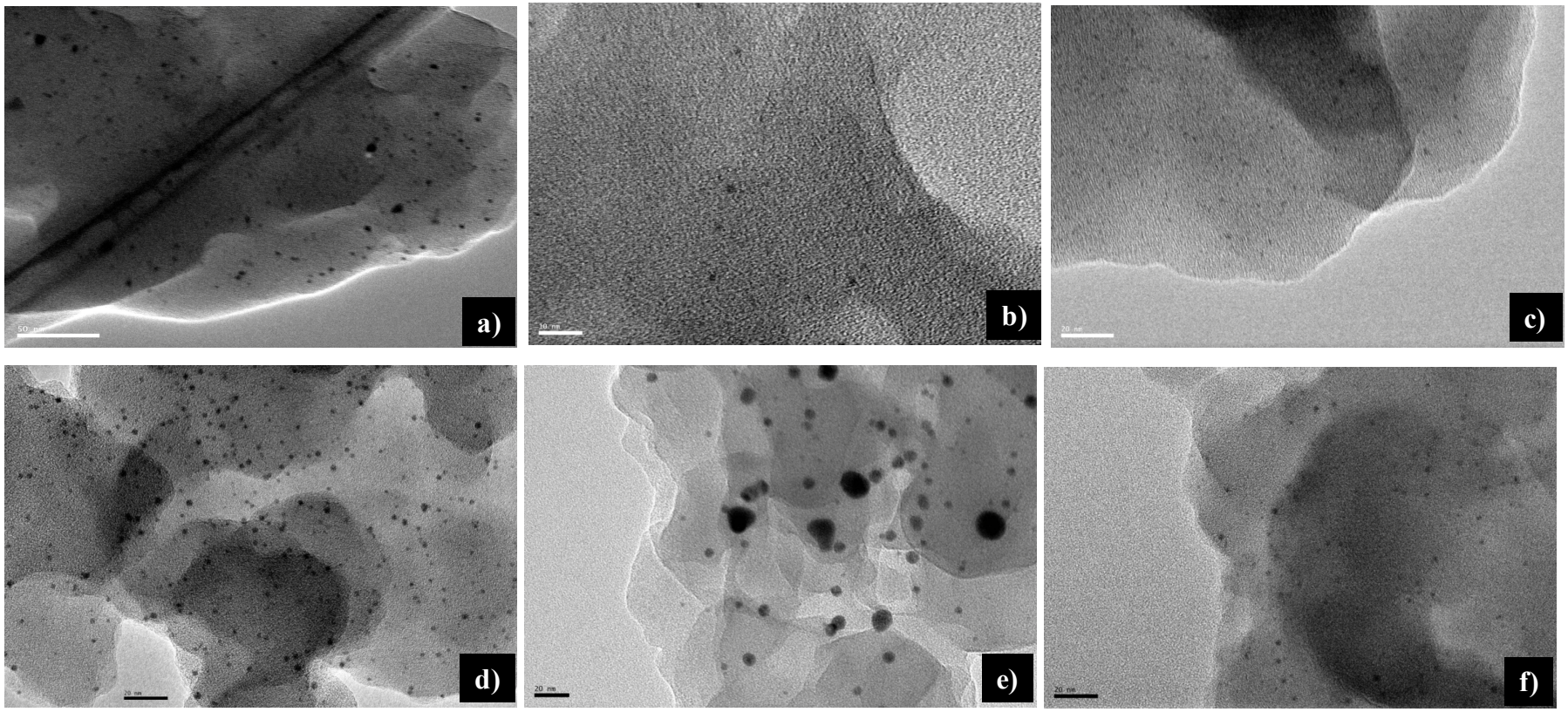

Figure S8. TEM imagines of different AuNPs-SILLPs prepared by theloading/reduction procedure from resins having a low loading of IL-like moieties: a) AuNPs-SILLP-**11c** (R=CH_3, R´=H) (bar 50 nm),, b) AuNPs-SILLP-**12c** (R=C_4H_9, R´=H) (bar 20 nm),, c) AuNPs-SILLP-**13c**, (R= $C_{10}H_{21}$, R´=CH_3) (bar 20 nm), d) AuNPs-SILLP-**11d** (R=CH_3, R´=H) (bar 20 nm),, e) AuNPs-SILLP-**12d** (R=C_4H_9, R´=H) (bar 20nm), and f) AuNPs-SILLP-**13d**, (R= $C_{10}H_{21}$, R´=CH_3) (bar 20 nm).

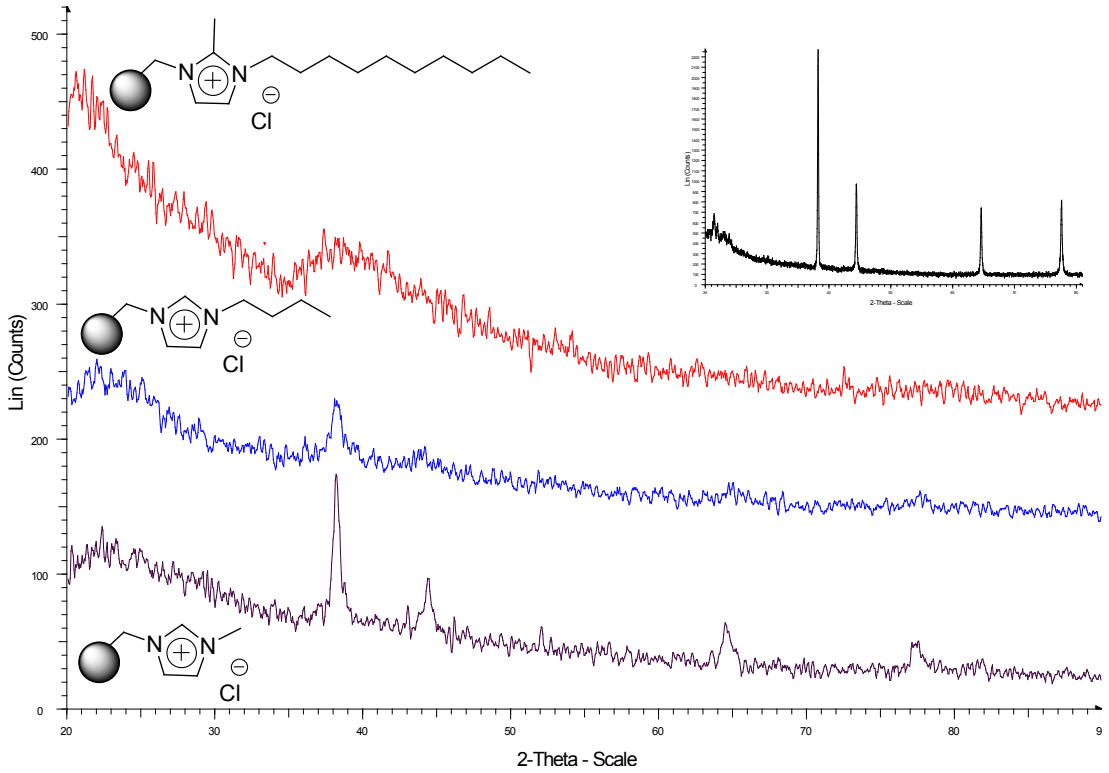

Figure S9. XRD spectra of AuNPs-SILLP-**11b** (R=CH_3, R´=H), AuNPs-SILLP-**12b** (R=C_4H_9, R´=H), and AuNPs-SILLP-**13b**, (R= $C_{10}H_{21}$, R´=CH_3) together with XRD spectra of pure Au(0) (inset).

Table S4. Long term stability of some AuNPs-SILLPs.[a]

Entry	AuNPs-SILLP	R	R`	λ_{max} [b] incial	λ_{max} [b] Final	Time (days)
1	**11c** (*g*)	CH_3	H	525	525	150
2	**12c** (*g*)	C_4H_9	H	530	530	150
3	**13c** (*g*)	$C_{10}H_{21}$	CH_3	528	528	150
4	**12b** (*m*)	C_4H_9	H	539	539	240

[a] gold loading of all AuNPs-SILLPs 0.05 mmol/g of support . [b] SPR for the AuNPs-SILLPs obtained after reduction

Equipment.

Optical microscopy

Optical microscopy observations were carried out using an optical microscope (epifluorescent) Optika N-400FL, with a trinocular head lighting system using an halogen bulb (6V/20W). Dry samples on a glass microscope slide were prepared by initial deposition on the glass microscope slide of a dispersion of the material in water (or required solvent) and further evaporation of the solvent. DTA and TG analyses were performed in a Mettler Toledo model SDTA 851e under an argon atmosphere. All experiments were run in a 150 mL Pt crucible from 25 to 500 ºC with a heating rate of 5 ºC min.

Scanning electron microscopy (SEM) The scanning electron micrographs were acquired using an electron microscope Leica-Zeiss LEO 440I with a LaB_6 thermoionic electron gun working at an accelerating voltage of 20kV with eight motorized specimen samples. The system was equipped with a digital camera and an Si(Li) EDX detector. The software used was the INCA 250 (Oxford package). The samples were metalized with carbon in a Polaron SC7610 foil of Fisons Instruments.

Transmission electron microscopy (TEM)

The transmission electron micrographs were acquired in an electron microscope JEOL 2100 with a (LaB6) thermoionic gun with a maximum acceleration voltage of 200KV and a maximum resolution of 0.14nm and 0.23 nm between points, coupled to a energy dispersive microanalysis system (EDS) TEM Inca Energy 200 (Oxford), with a resolution of 136eV with a detection range from B to U. The system was equipped with a high resolution (11Mpixels) CCD camera for image acquisition, Orius model (Gatan) integrated within the program of acquisition and image processing (Digitall Micrograph

package, Gatan Inc.). The samples were dispersed in ethanol by sonication and speckled on a copper grid coated with amorphous carbon film.

X-ray powder diffraction

Two equipments were employed for data acquisition: i) D4 Endeavor, Bruker-AXS powder diffractometer with theta/2theta Bragg-Brentano geometry, copper X-ray tube, diffracted beam monochromator and scintillation detector. Data were collected by step-scanning from 20 ° to 90 ° 2θ with a step size of 0.02 ° 2θ and 2 sec. of counting time at each step; ii) D8 Advance, Bruker-AXS powder diffractometer with theta/2theta Bragg-Brentano geometry, with primary Ge monochromator, copper X-ray tube and a scintillation detector using a capillary for samples measurement. Data were collected by step scanning from 20 ° to 90 ° 2θ with a step size of 0.02 ° 2θ and 10 sec. of counting time at each step. The results obtained were analysed using EVA (Bruker-AXS) computer software which determined diffraction peak positions and intensities and the JCPDS database of the International Centre for Diffraction Data (PDF-2 release, 2003) for the identification crystalline phases.

Diffuse reflectance spectrophotometry UV-Vis (DRS).

Diffuse reflectance spectra were performed with a Cary 500 Scan spectrophotometer (Varian), using an integrating sphere and $BaSO_4$ as a reference. The data were registered from 380 to 700 nm using a glass blank (glass microscope slide) as reflecting standard and a D65 standard illuminant.

Absorption spectrophotometry UV-Vis.

UV–vis absorption spectra were recorded in a Hewlett- Packard 8453 apparatus.